A CRACKING MODEL FOR PLAIN JOINTED PORTLAND CEMENT CONCRETE PAVEMENTS

D.R. MacLeod, Carleton University, Canada,
formerly University of California, Berkeley
C.L. Monismith, University of California, Berkeley

This paper examines the relationships between two modes of distress and performance for plain, jointed portland cement concrete without dowels at transverse contraction joints. The two modes examined are joint faulting and cracking which are major contributors to loss in serviceability for well designed and constructed pavements in California. Analysis of 500 lane miles of faulted pavement indicates that faulting is related to the number of EALs and that the type of cement-treated material influences faulting behavior. Guidelines are presented for prediction of faulting distress. Cracking analyses using finite element procedures indicate that the strength of the cement-treated layer has an important effect on fatigue life of pcc pavements. Detailed traffic analyses of 600 lane miles of pavement in the San Francisco Bay Area, considering thermal stresses and material variations, indicate that there is a common fatigue relationship for pcc pavements when the fatigue relationship: $n_f = 225{,}000 \left[\frac{M.R.}{\sigma}\right]^4$ is used. The analyses also indicate that there is little time differential between the onset of first and third stage cracking. Once 20 percent of the slabs show first stage cracking, the serviceability of the pcc pavement is terminating. Analyses indicate that this performance model is also applicable to other environments in California. The results of the study are used to illustrate the framework for a rehabilitation management system for plain, jointed pcc pavements.

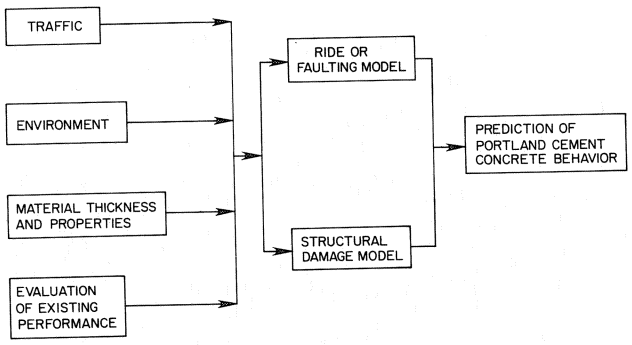
To establish an effective pavement management system for portland cement concrete (pcc) pavements, relationships between distress and in-service performance must be established. While there are a number of types of pcc pavements which must be considered, this discussion is limited to plain, jointed pavements without dowels at transverse contraction joints, a type common in the western United States and the only type used in California. The performance data were obtained primarily from heavily traveled state highways located in the San Francisco Bay Area although the study included state highways from other climatic environments in California as well.

While there are many different ways in which pcc can exhibit a loss in serviceability with time and traffic, three major problems were identified for well-designed and constructed plain-jointed pavements in California. These are: (1) lossin ride quality due to faulting; (2) extensive cracking or slab breakup; and (3) potential for hydroplaning due to loss of surface texture.

Of these, hydroplaning is the most easily managed with existing technology (1). Hence this discussion will be limited to the development of models for faulting and cracking.

Specifically, the investigation examined the relationship between faulting, rough ride, and traffic, and the relationship between slab cracking and traffic. Included are the effects of material properties, thicknesses of pavement components and climate. Figure 1 represents the framework for the performance models described herein. The two mechanisms may either separately or in combination contribute to reduced performance.

Figure 1. Framework for behavior prediction.



Pavement Roughness and Faulting

In this study, two procedures were used initially to define pavement roughness and faulting. One definition was by means of a ride score obtained by means of a PCA response type road meter developed by Soil Test Inc. and used by the California Department

of Transportation (CALTRANS) to provide data from an inventory procedure for use in their rehabilitation management system (2). Ride score is defined as:

$$\text{Ride Score} = \frac{\text{sum of road meter counts*}}{50 \times \text{odometer length (mi)}} \times \text{vehicle factor} \quad (1)$$

(*The sum of the road meter counts is obtained by adding together the products of the number of counts of 1/8 in. × 1, 2/8 in. × 2, 3/8 in. × 3, etc.)

This parameter is determined at a vehicle speed of about 85 km/hr (50 mph). When the ride score reaches a prescribed level, remedial action of some form is required.

The second definition was by means of a faulting index evaluated by a panel of raters on a scale of 0 to 10. When faulting reached a value of six on this scale, the raters generally agreed that remedial action was required.

On a mass inventory basis, because of lack of information on grinding, type of base course, inadequate traffic information, etc., no correlation between ride score and traffic could be obtained. For specific sections, however, for which maintenance history and base type were known, ride scores deteriorated (increased) with increasing 80 kN (18,000 lb) equivalent axle loads (EALs), e.g., Fig. 2.

Figure 2. Ride score vs EALs.

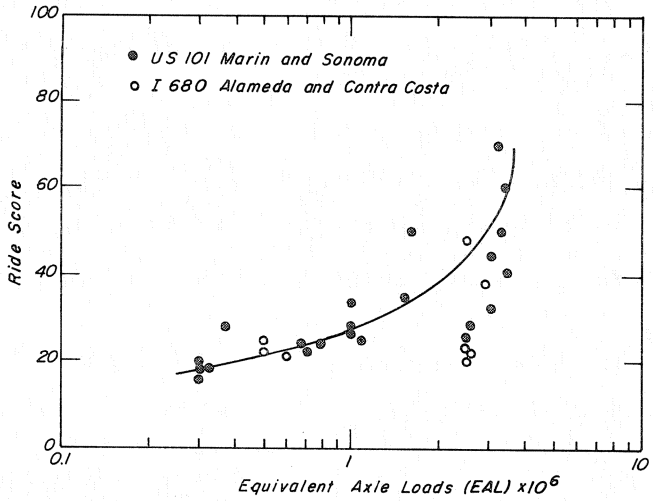
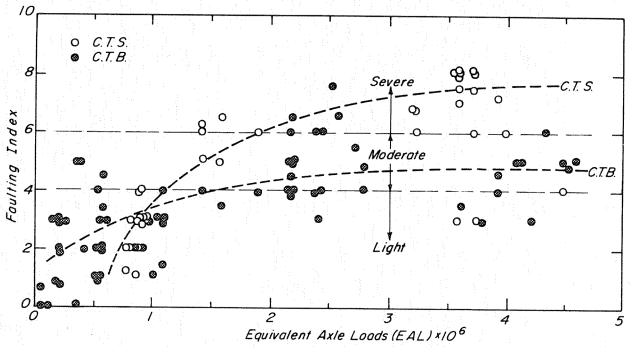


Figure 3 contains the results of the faulting index evaluations for two types of pavements, one with cement-treated base (CTB) and the other with cement-treated subgrade (CTS). The CTS generally contains more fines with a lower cement content than CTB; this material was used prior to CTB in California. While the scatter makes interpretation difficult, the CTB sections appear to perform better than CTS sections.

Figures 4 and 5 contain data obtained for various pavements in the San Francisco Bay Area. From this information the following guidelines seem appropriate:

1. For pcc pavements on CTS:
   a. Moderate faulting can be expected after 1.0×10^6 EAL repetitions.
   b. Severe faulting is not expected before 1.5×10^6 EAL repetitions.
   c. On the average, severe faulting can be anticipated at approximately 2.5×10^6 EAL repetitions.
2. For pcc pavements on CTB:
   a. Moderate faulting can be expected after 1.0×10^6 EAL repetitions.
   b. Severe faulting is not expected before 2.0×10^6 EAL repetitions.
   c. On the average, severe faulting can be anticipated at approximately 4.0×10^6 EAL repetitions.

Figure 3. Faulting index vs equivalent axle loads: U.S. 101 Marin and Sonoma counties.



Based on 1977 traffic figures, the difference in performance between pavements with CTB and CTS is approximately 2 to 3 years.

Figure 4. Faulting index vs equivalent axle loads for pcc pavements on CTS bases.

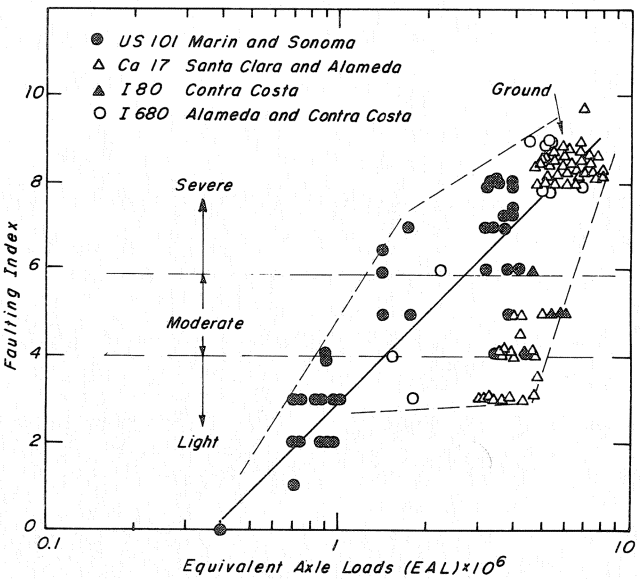


Figure 5. Faulting index vs equivalent axle loads for pcc pavements on CTB bases.

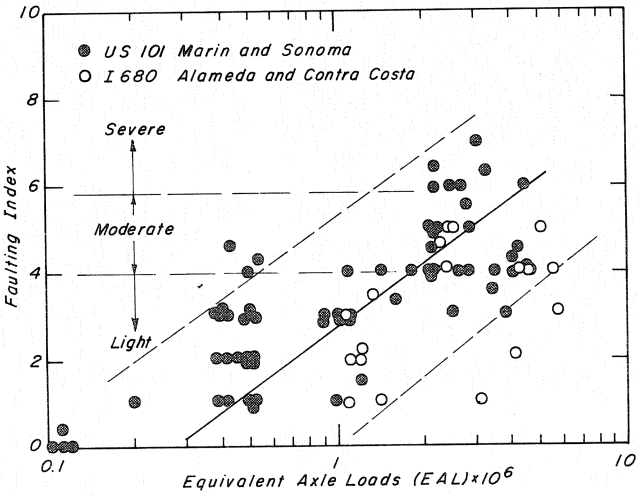
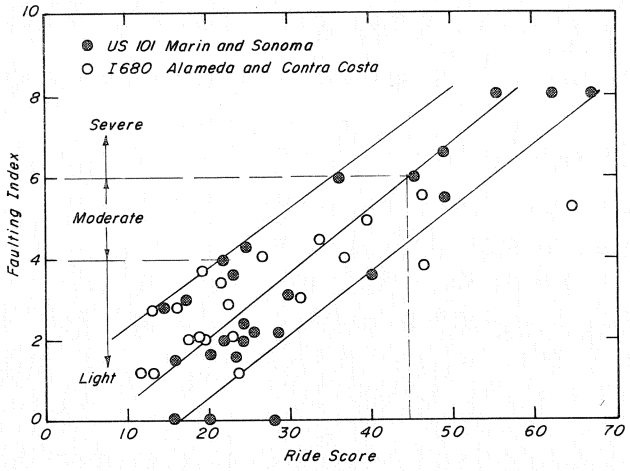


Figure 6 shows the correlation between ride score and faulting index suggesting that the road meter does measure faulting. As noted earlier, it was indicated that the majority of raters believed that remedial action was required when the faulting index was equal to or greater than six. This corresponds to an average ride score of forty-five, a value arrived at by CALTRANS in an independent study (2).

The information in terms of traffic and ride score (or faulting index) thus provides the necessary guidelines for predicting faulting distress for pcc pavements.

Figure 6. Ride scores vs faulting.

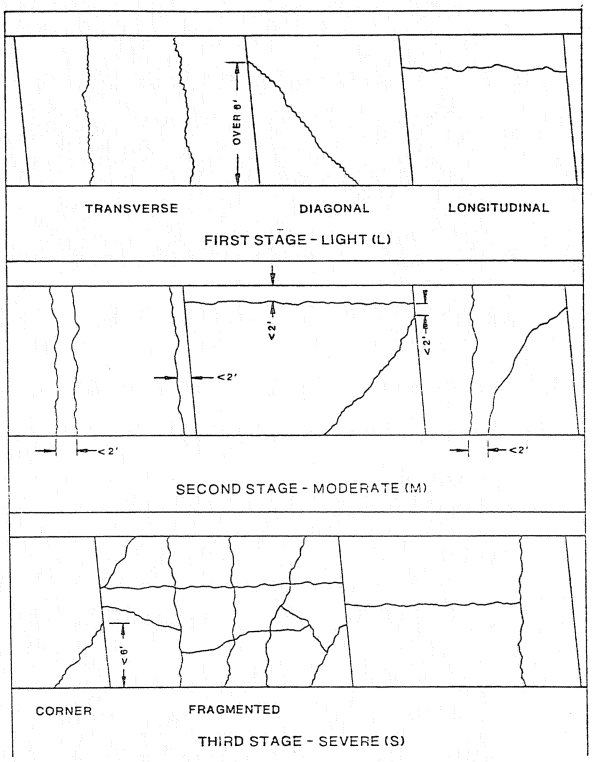


Pavement Cracking

To define pavement cracking, the procedure developed by CALTRANS (2) and shown in Fig. 7 was utilized. (Pavements investigated on this project displayed only a very limited amount of second stage cracking; therefore second stage cracking has been included with third stage cracking.)

Cracking data obtained from condition surveys by CALTRANS personnel in 1978 were utilized. These data were modified where appropriate (some differences were obtained emphasizing the necessity for cross checks and careful supervision of data collection) by one of the authors of this paper utilizing field observations and low-level aerial photography.

Figure 7. Stages of cracking (after CALTRANS (2)).



Influence of Traffic on Cracking

With the cracking information and traffic data, an attempt was made to ascertain if there existed a general relationship between the amount of cracking and traffic as measured by EALs for the various pavement sections. Figures 8a and 8b illustrate such data.

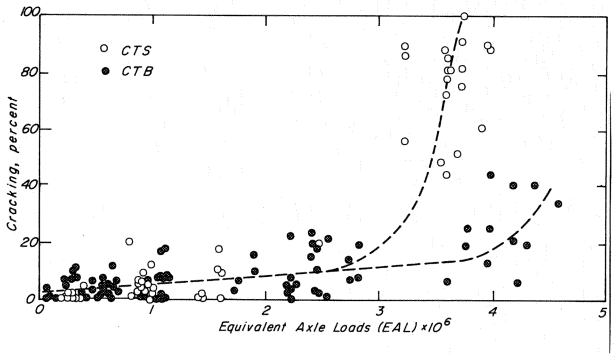
From this data, two distinct failure patterns are observed. Pavements designed utilizing CTS exhibit an acceleration in cracking between 3×10^6 and 3.5×10^6 EAL repetitions while pavements with CTB are performing adequately at beyond 4.0×10^6 EAL repetitions.

The data in Fig. 8b indicate that there is not a large time span between the onset of significant first stage cracking and the start of significant third stage cracking.

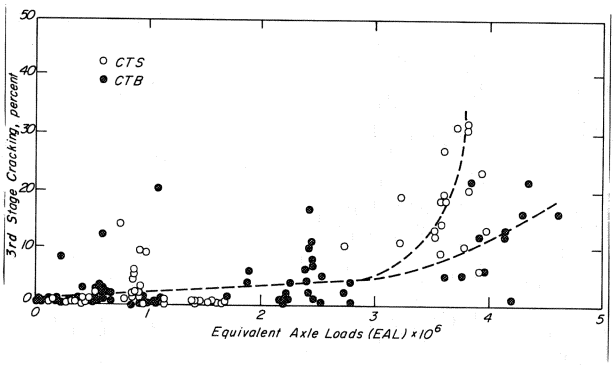
These data indicate that cracking cannot be related to traffic alone but such factors as pavement material characteristics [Pavements with CTS materials (generally less stiff than CTB materials) cracked transversely, while pavements with CTB showed considerably more longitudinal cracking. These longitudinal cracks generally started in the inner wheel path of the outer lane at the transverse joint and proceeded away from the joint until the slab was completely cracked.] and thicknesses and possibly climate may be significant in establishing pavement behavior. Accordingly, a mechanistic approach has been developed and is described in the following sections.

Figure 8. Cracking vs EALs - Sections One and Two.

a. Total cracking.



b. Third stage cracking.



Performance Model to Represent Cracking

A mechanistic model in which the various components of the pavement structure are assumed to be elastic in response has been utilized to develop the performance model. Figure 9 illustrates the procedure followed.

Laboratory testing of representative samples of in-situ materials and an evaluation of construction data were done concurrently with analyses of the pavement structures using a two-dimensional axisymmetric finite element configuration. These "sensitivity" analyses permitted the identification of significant material characteristics for use in the more expensive three-dimensional finite element analysis, this being necessitated by the finite dimensions of the concrete slabs. Only a few solutions were obtained for the three-dimensional configuration to establish the location of critical load stresses. The two-dimensional plane strain finite element analysis was then used to estimate stresses for the range in loads and material stiffness characteristics appropriate to the pavement sections. In these analyses, stresses were determined for a range in loads during five periods of a representative day for each of twelve months of the year. This approach permitted consideration of the superposition of temperature on load stresses. By comparing the linear sums of the cycle ratios for the various sections to the amount of cracking observed in the condition surveys, a performance model for load associated cracking was developed.

Pavement Sections. A major state highway, U.S. 101 in Marin and Sonoma Counties, was selected for the initial development since it displayed a range in distress severity, was subjected to a range in traffic loadings, was composed of different structural pavement sections and was in a comparatively uniform climatic environment. In addition, reasonable traffic data and construction records were available.

One section was constructed in 1957 and consisted of 200 mm (8 in) of pcc, 100 mm (4 in) of CTS and 150 mm (6 in) of untreated aggregate subbase (ASB). The other section, constructed in 1965, included 200 mm (8 in) of pcc, 100 mm (4 in) of CTB and untreated aggregate subbase ranging from 150-600 mm (6 to 24 in) in thickness.

Material Characteristics. Material characteristics were established from tests on a limited number of field samples and a detailed examination of the construction files.

Repeated load triaxial compression tests were performed on specimens of both the subgrade and subbase materials compacted in the laboratory to be representative of in-situ conditions. Table 1 contains a summary of the representative values selected for the analyses.

Stiffnesses of the cement-treated materials were estimated utilizing data from the construction files and the relationship:

$$\text{Stiffness (psi)} = 33(W)^{1.5}(UC)^{0.5} \qquad (2)$$

where: W = unit weight of concrete, pcf

UC = unconfined compressive strength, psi

Recognizing that in-situ strengths are less than those measured in the laboratory, laboratory measured strengths measured at the time of construction were reduced by one-third (10) for use in Eq. (2). In addition, specimens obtained from core samples were tested using a repeated load diametral modulus device.

Tables 1 & 2 contain a summary of the results. In pavement Section One, it will be noted that the measured values are substantially less than the estimated values. If the minimum strength required by specifications, 2.07 GPa (300 psi), is used in Eq. (2), an estimated value closer to the measured values is obtained.

Moduli for the pcc were estimated using construction data and Eq. (2) and were also measured on core specimens using the diametral device. Moduli of rupture were estimated from construction data using the expression:

$$\text{Modulus of rupture (MR)} = 9(f'_c)^{0.5} \qquad (3)$$

where: f'_c = compressive strength, psi

and also estimated from the diametral tests. Tables 1 and 2 contain a summary of these data.

Table 3 contains a listing of the parameters used in the analysis and includes estimated thermal characteristics as well as stiffness and strength values.

Figure 9. Steps in the definition of a fatigue realtionship for plain jointed pcc pavements.

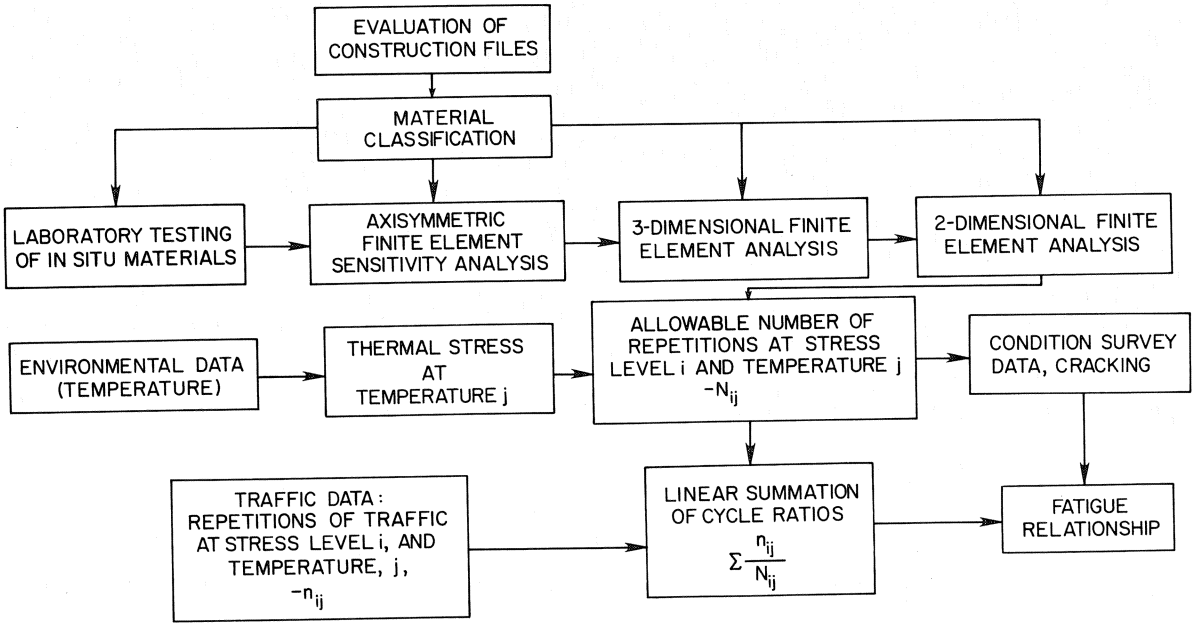


Table 1. Properties of cement-treated materials.

		Section One (CTS)		Section Two (CTB)	
		Construction Data			
Density	Mean	1,826 kg/m^3	114 pcf	2,339 kg/m^3	146 pcf
	Standard deviation	24.0	1.5	48.1	3.0
	Number of tests	16		12	
Seven day compressive strength	Mean	460 MPa	665 psi	491 MPa	711
	Standard deviation	153	221	54	78
	Number of tests	21		12	
		Estimated Stiffnesses			
Stiffness from equation (2)	Mean	5.8 GPa	0.84 × 10^6 psi	8.6 GPa	1.25 × 10^6 psi
	90 percent interval	6.2	0.90	8.8	1.28
	10 percent interval	5.5	0.79	8.5	1.23
	Using minimum strength, 300 psi	3.9	0.57		
		Measured Stiffnesses			
Stiffness from "undisturbed" samples (4 specimens)		1.0 GPa	0.14 × 10^6 psi	5.5 GPa	0.79 × 10^6 psi
		2.3	0.34	7.7	1.12
		1.9	0.28	8.0	1.16
		4.1	0.59	7.1	1.03

Table 2. Properties of portland cement concrete (pcc).

		Section One (CTS)		Section Two (CTB)	
Construction Data					
Density	Mean	2,387 kg/m^3	149 pcf	2,451 kg/m^3	153 pcf
	Standard deviation	20.8	1.3	12.8	0.8
	Number of samples	8		14	
Twenty-eight day compressive strength	Mean	21.7 MPa	3,144 psi	28.7 MPa	4.164 psi
	Standard deviation	3.2	465	3.5	505
	Number of Samples	5		31	
Stiffnesses					
Modulus from Equation (2)	Mean	23.1 GPa	3.35 × 10^6 psi	27.9 GPa	4.04 × 10^6 psi
	90 percent interval	24.0	3.48	28.2	4.09
	10 percent interval	22.2	3.22	27.6	4.00
Measured, diametral modulus	Mean	20.7	3.00	27.2	3.94
Modulus of Rupture					
Estimated from Equation (3)	Mean	3.48 MPa	505 psi	4.00 MPa	580 psi
	90 percent interval	3.59	520	4.04	585
	10 percent interval	3.38	490	3.97	575
Measured, diametral	Mean	3.10	450	3.90	565
	Range		-	2.97 - 4.76	430 - 690

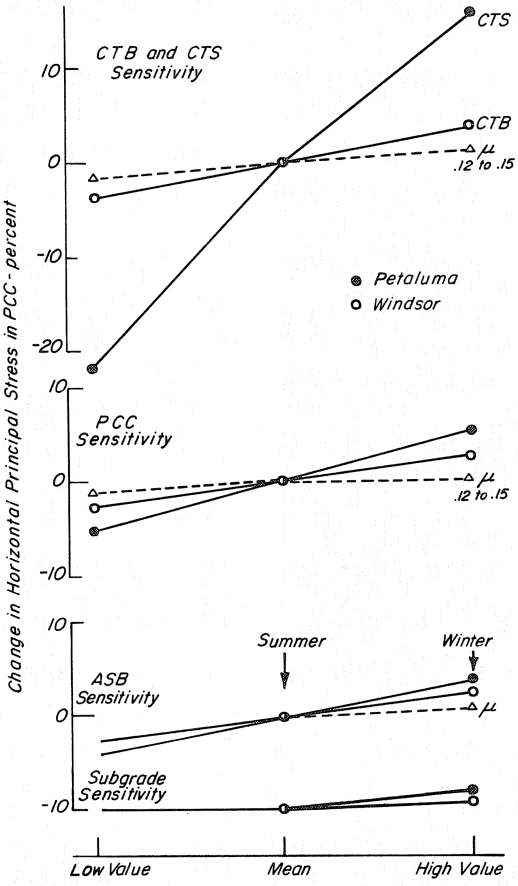
Table 3. Engineering parameters used to develop performance model.

		Section One (CTS)		Section Two (CTB)	
Portland cement concrete (pcc)					
Modulus of elasticity,	high	22.0 GPa	3.2 × 10^6 psi	29.0 GPa	4.1 × 10^6 psi
	mean	20.7	3.0	27.6	
	low	19.3	2.8	26.9	
Modulus of rupture,	high	3.58 MPa	520 psi	4.15 MPa	600 psi
	mean	3.45	500	4.00	580
	low	3.31	480	3.86	560
Cement-treated material					
Modulus of elasticity,	high	3.8 GPa	0.55 × 10^6 psi	8.3 GPa	1.2 × 10^6 psi
	mean	2.4	0.35	7.6	1.1
	low	0.7	0.10	6.2	0.9
Poisson's ratio		0.15		0.15	
Thermal expansion coefficient		9.0 × 10^{-6}/°C		9.0 × 10^{-6}/°C	
Aggregate subbase					
Resilient modulus,	summer (dry)	62.0 MPa	9,000 psi	103 MPa	15,000 psi
	winter (wet)	34.5	5,000 psi	69.0	10,000 psi
Poisson's ratio		0.35		0.35	
Subgrade					
Resilient modulus,	summer (dry)	49.7 MPa	7,500 psi	55.2 MPa	8,000
	winter (wet)	27.6	4,000	34.5	5,000
Poisson's ratio		0.35		0.35	

Sensitivity Analysis. A sensitivity analysis was conducted to ascertain the influence of material characteristics on the horizontal principal stress on the underside of the pcc since it is considered to be a reasonable damage determinant for fatigue cracking. The use of a two-dimensional axisymmetric finite element analysis permitted the parameters with the largest influence to be ascertained at relatively small cost.

Results of these analyses using the values from Table 3 are shown in Fig. 10. The stiffness characteristics of the cement-treated layer are seen to have the most significant influence for the range in materials examined.

Figure 10. Sensitivity analysis of pavement components.



Determination of Critical Stresses. The three-dimensional finite element program (SOLID SAP) was used to determine critical stresses since it has the potential to realistically represent the plain jointed concrete pavement structure. Because of cost only two cases were analyzed, winter conditions for both Sections One and Two and only the average values for the various stiffness characteristics were utilized.

Load was applied to two axles with 7 ft center to center spacing [This axle spacing was chosen even though it exceeds the average of 1.2 m (4 ft) used in California so that the axle configuration could be considered as single axles to permit comparison of loading at the transverse joint and mid-slab.]; each axle consisted of two tires with 40 kN (900 lbs) applied to each. The outer tire on each axle was positioned one ft from the edge of the slab.

Figures 11 and 12 indicate that the maximum stress occurs at the mid-slab edge, where the principal stress is approximately ten percent higher than the mid-slab interior stress. These stresses are larger than the corner stress and the stress at the interior wheel at the transverse joint.

The analysis also indicated that the S_{xx} stresses (tensile stresses in the x and y directions respectively) are larger than the S_{yy} stresses for loads located at mid-slab, indicating that transverse cracking in the mid-slab area should be the failure mode. Observed failures in Section One (CTS) confirm this. In Section Two (CTB), the magnitude of the S_{xx} stresses were only slightly larger than the S_{yy} stresses, such that different joint conditions could possibly lead to longitudinal cracking.

Since the largest stresses occur at the mid-slab loading, it is possible to simplify the analysis using a two-dimensional finite element plane strain model along the y-y axis (Fig. 12) representative of the stresses caused by an axle at this location.

Figure 11. Principle stresses (psi) on underside of pcc - Section One. (1 psi = 6.9 KPa)

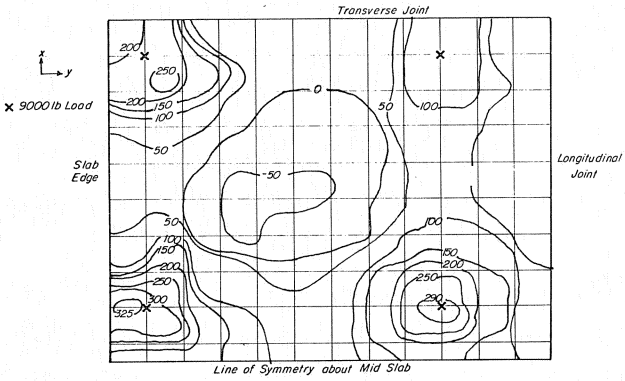
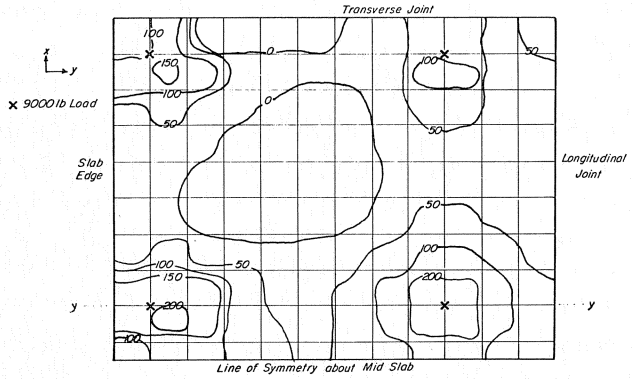


Figure 12. Principle stresses on underside of pcc - Section Two. (1 psi = 6.9 KPa)

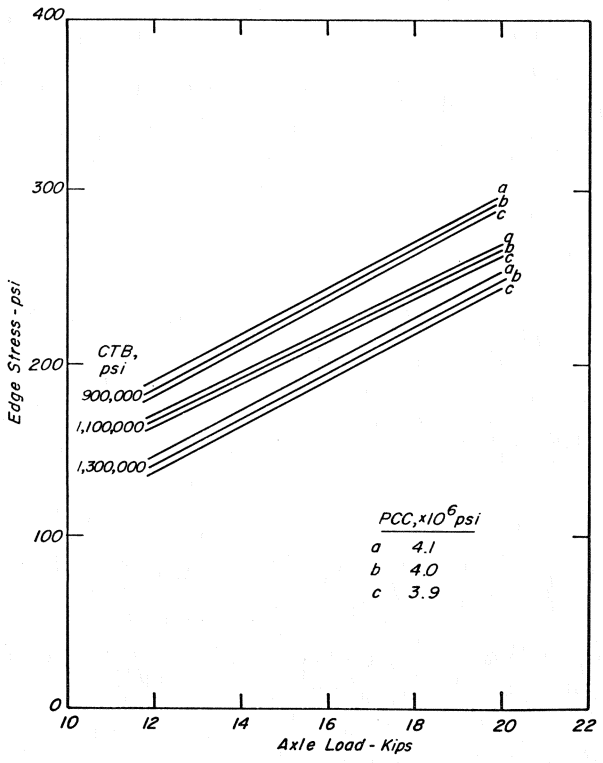


Load Stress Analyses. From the two-dimensional solution, stresses in the concrete were determined for a specific axle load and subgrade condition for the range in stiffnesses for both the cement-treated and pcc layers. Figure 13 is one such example of the results of these computations for Section One. [The three-dimensional finite element program and results published in Ref. (3) indicate that stresses resulting from a load placed about one ft from the pavement edge are approximately ten percent higher than stresses from a load in the interior of slab. Accordingly, the interior stresses calculated with the two-dimensional program have been increased to obtain the edge stresses.]

For Section Two, differences in the quality and thickness of pcc (10 psi stress differences) and changes in winter and summer subgrade stiffnesses (±5 psi stress differences) do not have a significant influence on pavement life. The mean value for pcc stress (CTB modulus = 7.6 GPa (1.1×10^6 psi)), pcc modulus = 27.6 GPa (4.0×10^6 psi)) in Fig. 13 represents eighty percent of all loading conditions. Another ten percent is represented by the upper confidence interval in CTB stiffness while the remaining ten percent is represented by the lower confidence interval of CTB stiffness.

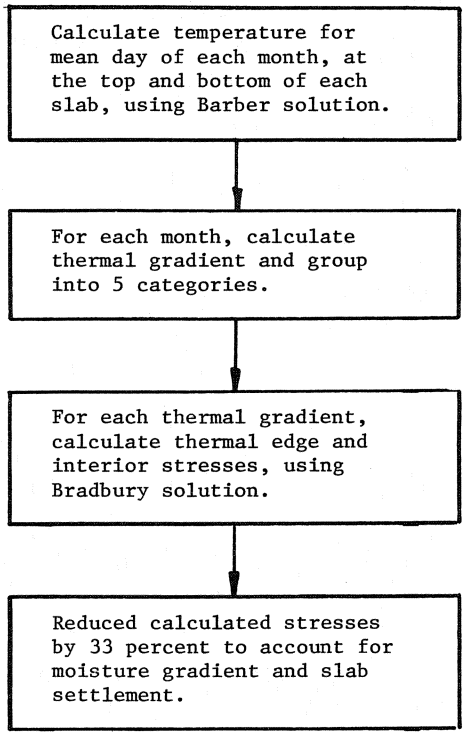
Similar conditions are representative for Section One; however, there were more significant differences between the effects of winter (October-March) and summer subgrade and subbase stiffnesses. The analysis was therefore subdivided into the two conditions.

Figure 13. Tensile strain on underside of pcc vs axle weight, Section Two, winter conditions. (1 psi = 6.9 KPa)



Temperature Stress Determinations. Temperature stresses were estimated for the two pavement sections using the procedure developed by Bradbury (4). Temperature gradients (five in number for a specific day in each month) were estimated by the Barber procedure (5) from weather data obtained from a station near the analysis sections. Figure 14 details a schematic representation of the procedure. Truck traffic is neither uniformly distributed throughout the day nor the month of the year. Accordingly, factors were developed to account for the distribution of trucks within these temperature gradients.

Figure 14. Calculation of thermal stress.



Cracking Analysis. The linear summation of cycle ratios cumulative damage hypothesis has been used to estimate the accumulation of damage for a range in axle loads and temperatures, i.e.:

$$\sum \frac{n_i}{N_i} \leq 1 \qquad (4)$$

where: n_i = number of load applications at stress σ_1

N_i = allowable number of load applications at stress, σ_i (from fatigue relationship).

Cracking is anticipated when this ratio approaches unity.

The specific fatigue relationship utilized for the pcc is that suggested by Vesic (6):

$$N_f = 225{,}000\left(\frac{MR}{\sigma}\right)^4 \qquad (5)$$

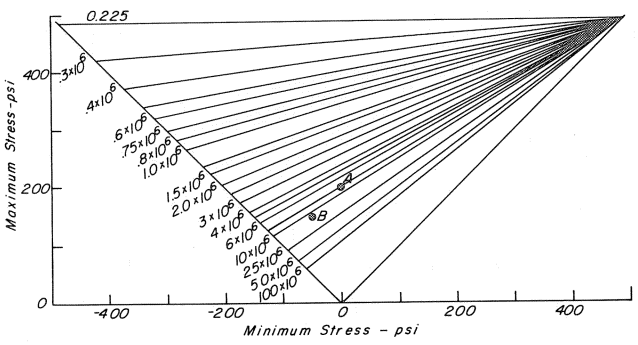
where: N_f = load applications to cracking

MR = modulus or rupture, psi

σ = tensile stress, psi

To consider the combined effects of load and thermal stresses, the Modified Goodman diagram (as suggested by Pretorius (7)) has been used, Fig. 15. As an example, consider a pavement system in which the tensile stress due to traffic loading is 200 psi (1.38 MPa). When the temperature gradient is 0, the fatigue life is approximately 8×10^6 applications; Case A, Fig. 15. For the situation in which a thermal stress is superimposed on the load stress, assume that the thermal stress is -53 psi (-0.37 MPa) (compressive - bottom of slab at higher temperature than top). For the same load stress, the fatigue life is about 15×10^6 repetitions; Case B, Fig. 15.

Figure 15. Modified Goodman diagram. (1 psi = 6.9 KPa)



The format for the complete analysis is shown in Fig. 16. Figs. 17 and 18 show the results of the analysis for both Sections One and Two.

Failure occurs when the Σ n/N exceeds unity and the curve in each figure applies to both sections, that is to both CTS and CTB designs. A comparison of Figs. 17 and 18 indicates that there is little time differential between the onset of severe first stage cracking and accelerated third stage cracking. Once twenty percent of the slabs exhibit first stage cracking, the service life of the pcc pavement is terminating. While there is some scatter in the data, the agreement is quite good. Scatter could be caused by local variations in traffic, local construction problems (poor joints), local subgrade problems (e.g., landslide), and settlements (invariably, the panels next to bridge structures are cracked).

Figure 19 contains the results of a similar analysis using the PCA fatigue criteria (8). Although indicating a fatigue relationship, these criteria are not satisfactory since there is little correlation between the two groups of data.

Thus it would appear that the approach embodied in Fig. 9 using a mechanistic analysis has provided a reasonable performance model. To examine the validity of this approach, a series of pavements from different locations in California were analyzed as described in the next section.

Applicability to Other Plain-Jointed Pavements in California

Sections for this analysis included other routes in the San Francisco Bay Area, together with sections from climates representative of the coastal, central valley, and mountain-desert areas of California. Details of these analyses are contained in Ref. (9); only the results will be briefly summarized herein.

Study Section Three -- San Francisco Bay Area (Interstate 680, Alameda and Contra Costa Counties). With the exception of Sections One and Two, this section included the most reliable data of the additional routes studied.

Comparison with Sections One and Two, Figs. 20 and 21, indicates reasonable agreement. This study section included pavements containing 9 in of pcc on CTB, 8 in of pcc in CTB, an 8 in of pcc on CTS making the comparison even more significant.

Study Section Four -- San Francisco Bay Area (Interstate 580, Alameda County). This section is a major route connecting the Bay Area to the San Joaquin Valley. Portions of this route near Oakland have restrictions in traffic (no trucks over four tons), and while these segments have experienced large traffic volumes, little cracking is evident.

Portions identified as climbing lanes are showing more distress; this is probably related to embankment settlement more than to fatigue, since both lanes are cracked.

Figures 22 and 23 illustrate the results of the analyses and indicate the validity of the cracking performance model.

Study Section Five -- California Coastal Environment, Southern California (U.S. 101, Santa Barbara County). Data for this study section also show good agreement with the criteria, Figs. 24 and 25. Certain segments have already been repaved with asphalt concrete and failure was predicted by the analysis for these sections.

Other Study Sections. Analyses for another section in the San Francisco Bay Area, and those in the Southern California desert. a Northern California mountainous area, and the central valley all illustrate similar reasonable comparisons with the performance models of Figs. 17 and 18. Details are contained in Ref. (9).

Relationship between Total Cracking and Third Stage Cracking

The data presented has indicated that cracking occurs when the summation of the n/N ratios approaches 1.1 to 1.4. The data also indicate that significant third stage cracking occurs when this ratio approaches 1.1 to 1.4.

Figure 26 compares the mean of the failure envelopes developed from Study Sections One and Two. At twenty percent total cracking, there is a difference of 0.3 to 0.4 in the Σ n/N to significant third stage cracking. As seen in Table 4, for a number of sections, 1977 traffic consumes approximately ten percent of the pavement life (0.1 n/N). With this as a guideline, the difference between twenty percent cracking and significant third stage cracking is approximately three to four years.

Relationship between EAL and n/N

The Σ n/N requires considerable time to determine; hence it would be desirable to have a relatively simple relationship between traffic (EALs) and this ratio. Figure 27 indicates that a unique relationship does not exist. Rather the relationship is controlled by axle weight distribution, climate, and structural section. This is not surprising since the EAL concept holds that the fraction or multiple

Figure 16. Steps in cracking analysis.

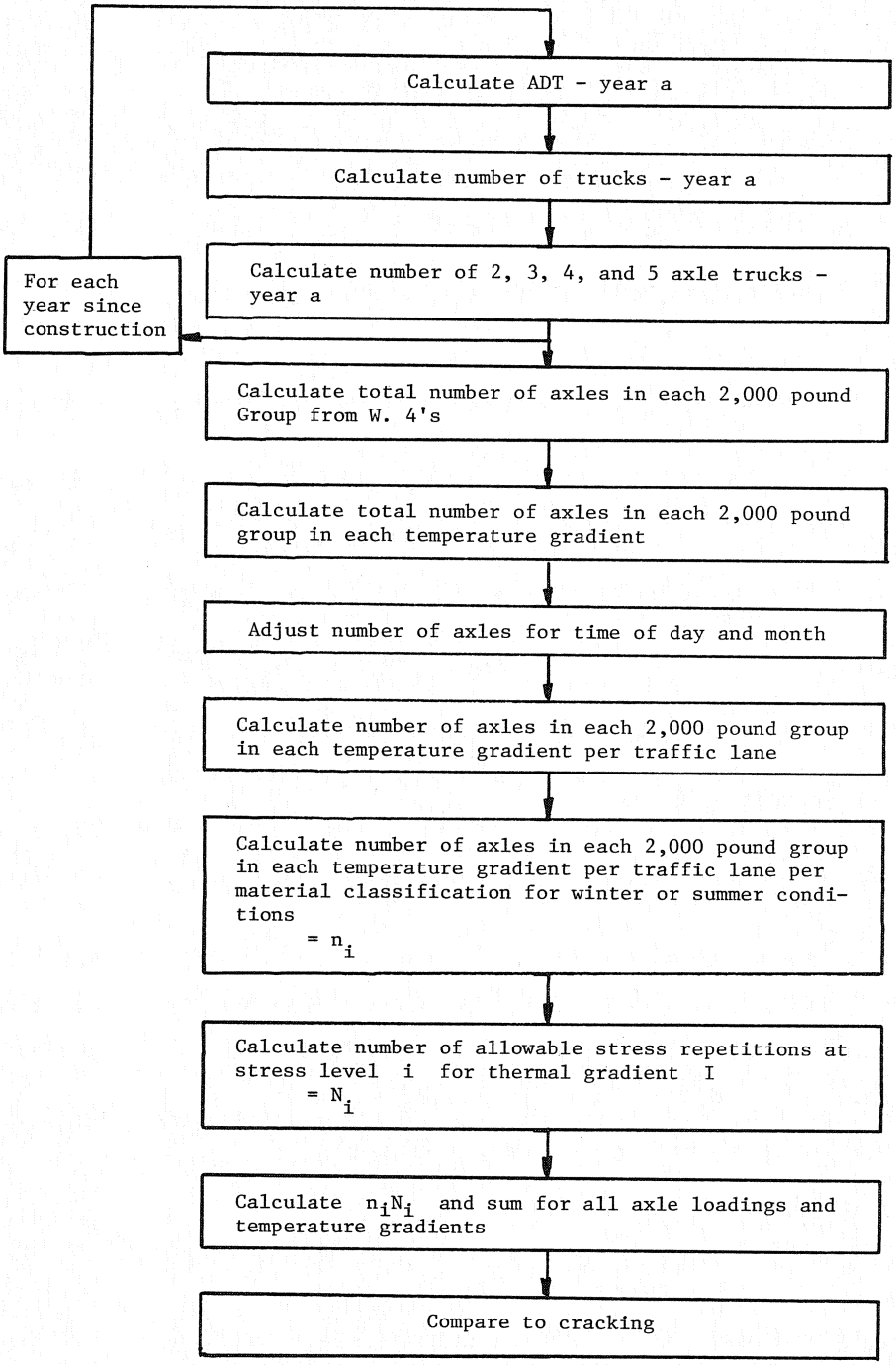


Figure 17. Total cracking vs n/N, Sections One and Two (US 101).

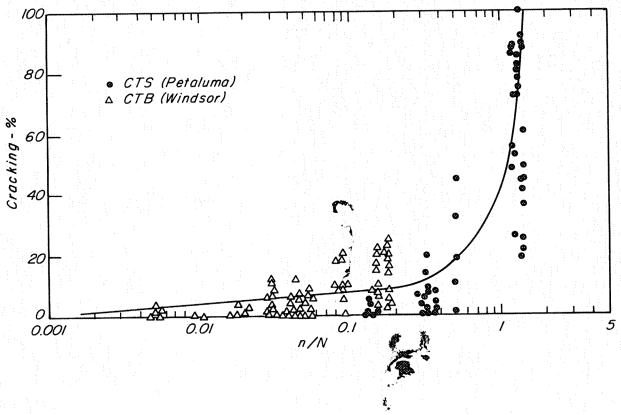


Figure 18. Third stage cracking vs n/N, Sections One and Two (US 101).

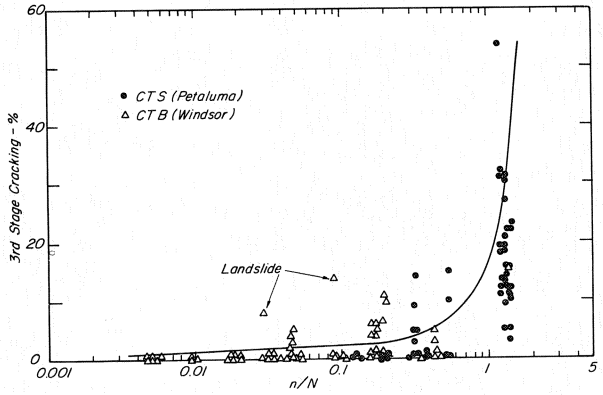


Figure 19. Total cracking vs n/N; PCA fatigue criteria.

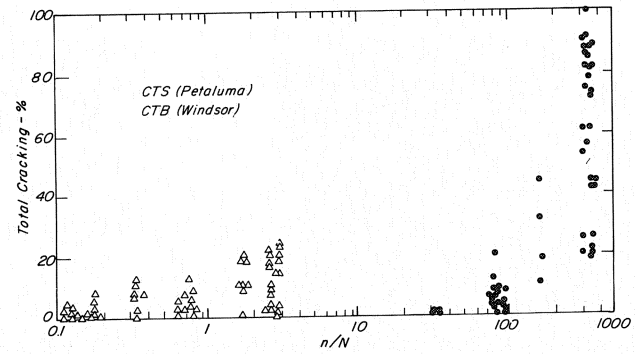


Figure 20. Total cracking vs n/N, Section Three (I 680).

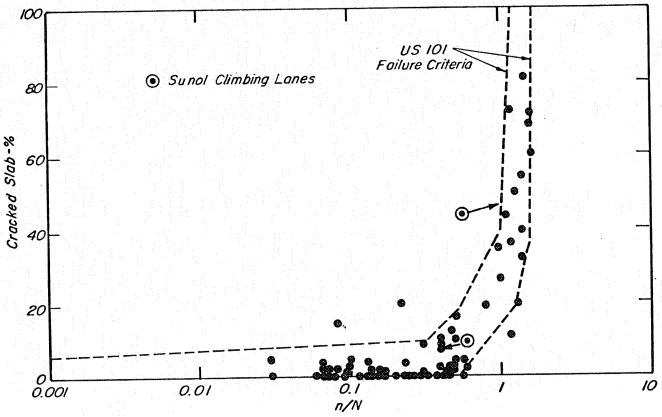


Figure 21. Third stage cracking vs n/N, Section Three (I 680).

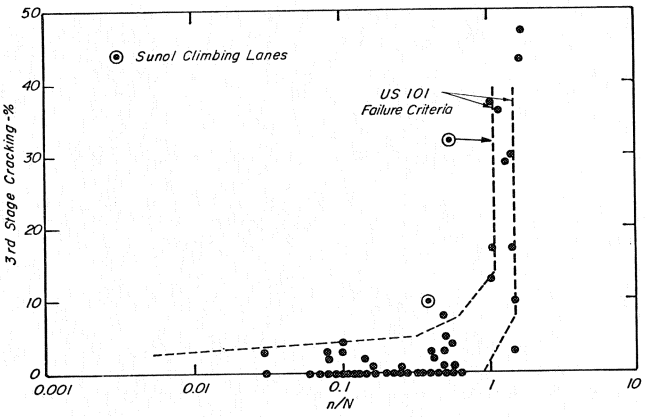


Figure 22. Total cracking vs n/n, Section Four (I 580).

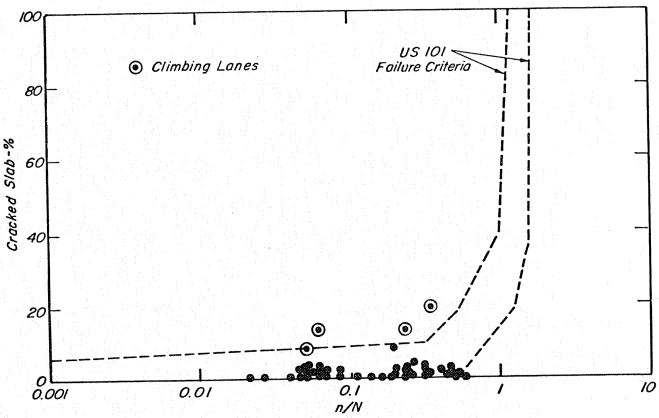


Figure 23. Third stage cracking vs n/N, Section Four (I 580).

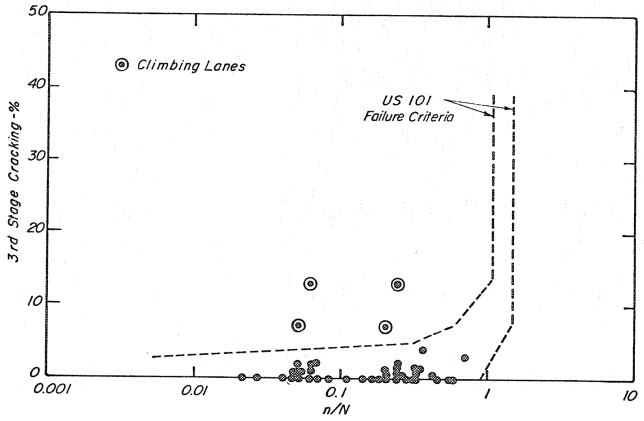


Figure 24. Total cracking vs n/N, Section Five (US 101).

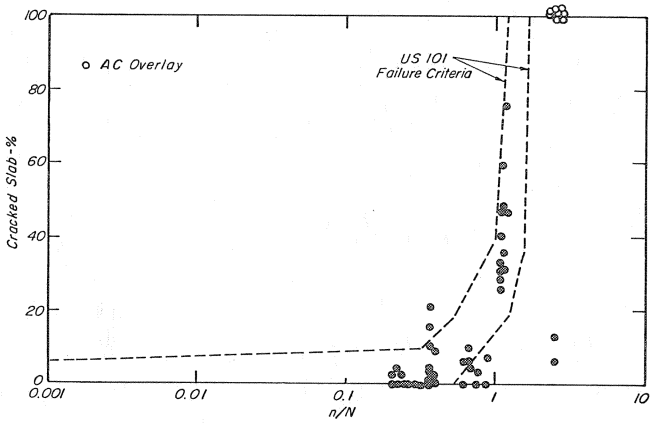
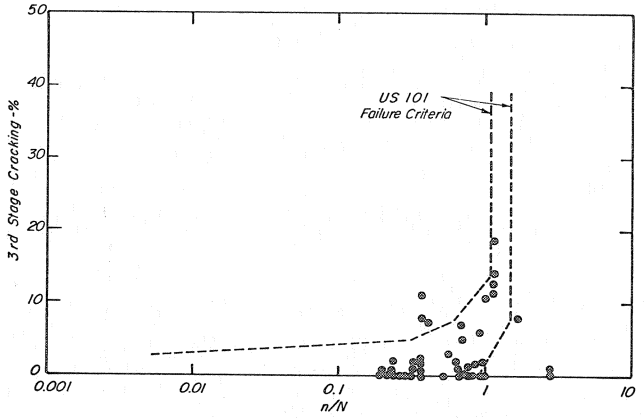


Figure 25. Third stage cracking vs n/N, Section Five (US 101).



of the load is the same (in terms of damage) for all situations. This is not true on a fundamental structural basis, hence the differences shown in Figs. 8a and b.

Relationship between the Occurrence of Faulting and Slab Cracking

Data in Table 5 have been produced from the information contained in Figs 4 and 5 and Fig. 26. As seen in this table, faulting becomes a problem before cracking does. For pavements with CTS, the difference in n/N is about 0.4 (about four years at 1977 traffic levels). For pavements constructed with CTB, the difference is larger, about 0.6 n/N (about six years of 1977 traffic levels).

Pavement Management Considerations

The results of the study can be utilized to develop a pavement management system for plain jointed pcc pavements. One such simple framework is illustrated in Fig. 28.

Considering this framework, pavements that are not faulted or cracked do not require major improvements. Of interest is how much longer they will continue to provide maintenance free service.

Pavements that are faulted but not cracked require rehabilitation if the excess user costs are greater than the costs of improving riding quality. In reality, these costs are the primary incentive to improve faulted pavements. If user costs are not considered, the "do nothing" alternative is a logical course.

Pavements which are both faulted and cracked should be compared on the basis of the combined excess user and maintenance costs, and the cost of rehabilitating the pavement. User costs are increased because of faulting, and maintenance costs are increased in an effort to keep the pavement in a serviceable state.

A fourth possibility is that the pavement is cracked but not faulted. In this case, the increased maintenance costs to keep the highway serviceable must be compared to the cost of rehabilitating the pavement.

Some of the implications of the results reported herein relative to this framework are:

1. On the average, the time span between the appearance of fifteen to twenty percent cracking and severe slab breakup is in the order of three to four years. This would indicate that new pavements need not be included for periodic pavement evaluation until they are five to six years old. When the cracking index is less than fifteen percent, a survey every second or third year should be adequate. Once cracking exceeds fifteen percent of the slabs, more frequent evaluations are required.
2. Faulting occurs before cracking in almost all cases. If there is less than fifteen to twenty percent cracking, grinding to improve the ride is a strategy to be considered in an economic analysis. If cracking is greater than fifteen percent, then grinding is of less value, since work to repair the cracked slabs would be necessary in the near future even if faulting were not a problem.

Figure 26. Mean cracking patterns vs n/N.

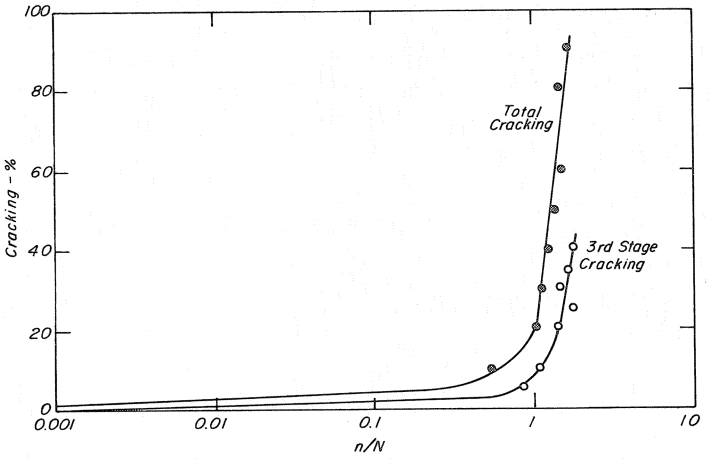


Figure 27. Relationship between EALs and n/N for various routes.

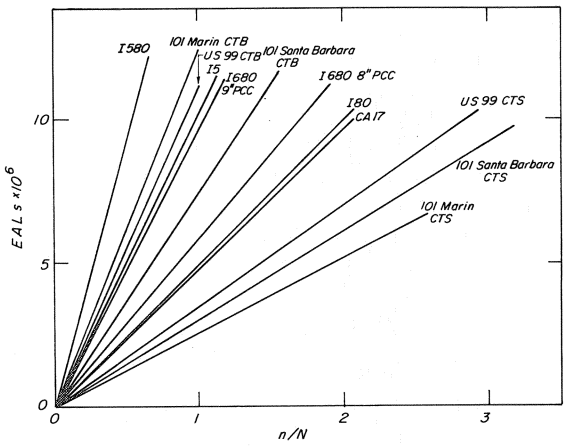


Figure 28. Framework for pavement management system for plain jointed pcc pavements.

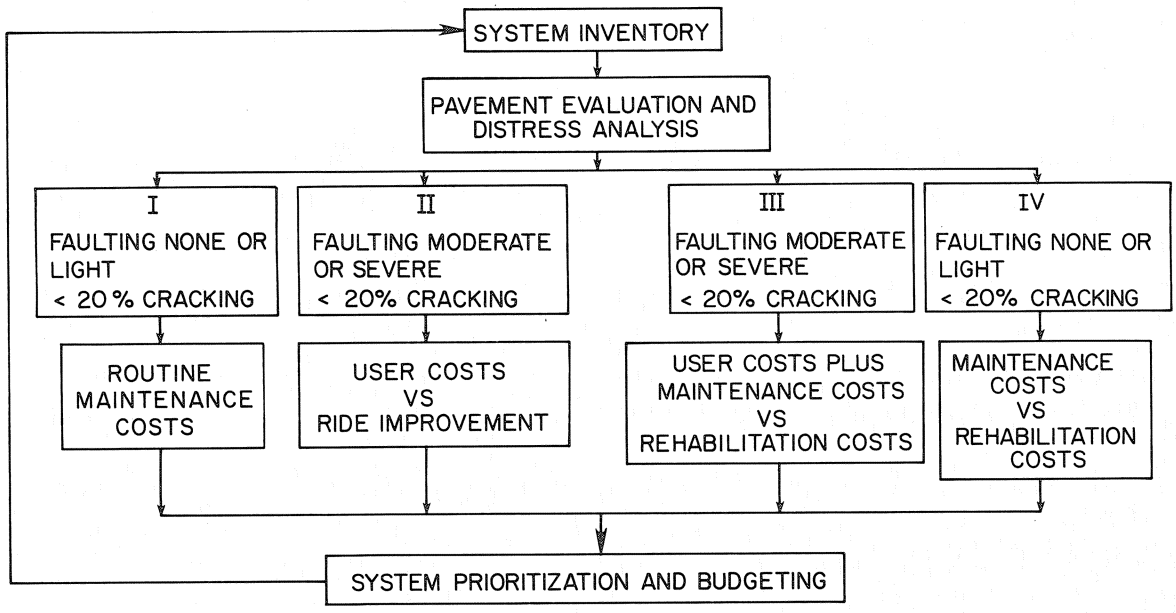


Table 4. Estimated proportion of fatigue life used on selected routes for the year 1977.

Route	County	n/N
Interstate 5	Siskiyou	0.096
U.S. 99	Tulare	0.104
U.S. 101	Santa Barbara	0.070
U.S. 101	Santa Barbara	0.081
Interstate 680	Contra Costa	0.096
Interstate 680	Contra Costa	0.093

Table 5. n/N to unacceptable distress levels.

Route	n/N to Severe Faulting	n/N to 20 percent Cracking
California 17	0.85	1.3
Interstate 80	0.90	1.3
Interstate 680	0.60	1.3
U.S. 101	1.0	1.3
U.S. 101	0.60	1.3

Acknowledgments

This study was conducted in cooperation with the Pavement Management System Task Force, State of California, Department of Transportation and the U.S. Department of Transportation, Federal Highway Administration. The contents of this paper reflect the views of the authors who are responsible for the facts and the accuracy of the data presented herein. The contents do not necessarily reflect the official views or policies of the State of California or the Federal Highway Administration. The paper does not constitute a standard, specification, or regulation.

References

1. Kampe, K., "The Relationship between Pavement Defects and Repair Strategies and Their Expected Lives," paper presented at WASHTO meeting, San Francisco, CA, June 1978.
2. Bartell, C. and K. Kampe, Development of the California Pavement Management System, Vol. I, System Description, Final Report, FHWA-CA-HM-7139-78-03, California Department of Transportation, Sacramento, CA, October 1978.
3. Darter, M., Design of Zero Maintenance Plain Jointed Concrete Pavements, University of Illinois, Urbana, IL, 1977.
4. Bradbury, R.D., Reinforced Concrete Pavements, Wire Reinforcement Institute, Washington, D.C., 1938.
5. Barber, E.S., "Calculation of Maximum Pavement Temperature from Weather Reports," Bulletin 168, Highway Research Board, Washington, D.C., 1957.
6. Vesic, A.S. and S.K. Saxena, "Analysis of Structural Behavior of Road Test Rigid Pavements," Highway Research Record No. 291, Highway Research Board, Washington, D.C., 1969.
7. Pretorius, P.C., Design Considerations for Pavements Containing Soil-Cement Bases, Ph.D. Dissertation, University of California, Berkeley, CA, 1969.
8. Portland Cement Association, Thickness Design for Concrete Pavements, Skokie, IL, 1966.
9. MacLeod, D.R., Considerations for Maintenance Strategies for Portland Cement Concrete Pavements, Ph.D. Dissertation, University of California, Berkeley, CA, 1979.
10. Meeker, A.G., CTB, Route 9, CALTRANS Report CA-DOT 72-3149-1.76-21, California Department of Transportation, Sacramento, CA, 1976.